

DETERMINATION OF WIND LOADS CAUSING FLUTTER EFFECTS

Ladislaus Lzwambuka¹
Email: llzwambuka@yahoo.de

ABSTRACT

A new method on the determination of wind forces by experimental means in a wind tunnel is discussed. The method reported herein is based on the identification methodology of model parameters under time response (i.e. time domain identification).

As a test model, a thin plate of cypress wood, elastically suspended in three degrees of freedom to represent the idealized form of a classical airfoil, for which theoretical wind load parameters exist, has been employed. Wind load parameters, experimentally obtained on the test model under the new method, are compared with the theoretical values of classical airfoils.

Advantages of the new method against the conventional methods are discussed.

Key words:

Flutter = elastic vibrations due to wind loads
Flutter instability = magnified elastic vibrations signifying the critical wind speed
System parameters = properties of a structure in natural modes
Wind Load Parameters = properties of a structure signifying the influence of wind load
Flat plate = idealized model with structural behaviour as a streamlined body
Time domain = responses on basis of time interval
Frequency domain = responses on basis of frequency interval

INTRODUCTION

Experimental identification of system parameters from time response was developed by Ibrahim (1973 and 1976) and its applicability proved to be very effective. Since then subsequent improvements of the method was made by Badenhausen (1985) and Ibrahim (1985) in terms of enhanced accuracy, resolution and anti-disturbance.

Until now experimental identification of model parameters were confined only to model vibrations in still air (natural model). In this paper the identification technique is being introduced to determine vibration parameters of a model under wind flow in a wind tunnel (aerodynamic model). The parameters obtained from testing the aerodynamic model are non-constant. They are dependent on wind speed and vibration frequency.

The primary objective of wind tunnel tests reported herein is to extract, from the aerodynamic model parameters, the influence of wind in the form of wind load derivatives. For this, the constant natural model parameters constitute reference values.

The previous method used to determine wind load parameters under free response was developed by Scanlan (1971 and 1975) and is widely used to predict flutter instability for long span bridges. With the method of Scanlan, wind load parameters were obtained under several test procedures depending on the number of vibration modes to be excited. Technical constraints as well as the adopted approximation techniques which form the essential part of the method had adverse effects on the accuracy of results obtained.

The method presented in this paper has the basic advantage in that the limitations inherent in the conventional method are eliminated. In this approach only one test procedure is required because the method is based on coupled modes of vibrations. The application of the method presented herein, however, is possible only by means of high speed digital computers and appropriate software.

2. BASIC ANALYTICAL PRINCIPLE

The motion of a structural object under wind action and assuming a steady flow is described through the following set of equations (1):

$$\underline{M}_s \ddot{\underline{U}} + \underline{D}_s \dot{\underline{U}} + \underline{K}_s \underline{U} = \underline{M}_w \ddot{\underline{U}} + \underline{D}_w \dot{\underline{U}} + \underline{K}_w \underline{U} \quad (1)$$

with

$$\underline{M}_s, \underline{D}_s, \underline{K}_s = \text{System Parameter Matrices}$$

$$\underline{M}_w, \underline{D}_w, \underline{K}_w = \text{Wind Load Parameter Matrices}$$

$$\underline{U} = \text{The Displacement Vector}$$

The fundamental similarities of both sides of eq.(1) allow one to re-write eq.(1) in the form of:

$$(\underline{M}_s - \underline{M}_w) \ddot{\underline{U}} + (\underline{D}_s - \underline{D}_w) \dot{\underline{U}} + (\underline{K}_s - \underline{K}_w) \underline{U} = \underline{O} \quad (2)$$

which can be simplified to read:

$$\underline{M} \ddot{\underline{U}} + \underline{D} \dot{\underline{U}} + \underline{K} \underline{U} = \underline{O} \quad (3)$$

with

$$\begin{aligned} \underline{M} &= \underline{M}_s - \underline{M}_w \\ \underline{D} &= \underline{D}_s - \underline{D}_w \\ \underline{K} &= \underline{K}_s - \underline{K}_w \end{aligned} \quad (4)$$

Eq.(3) is homogenous and defines a free response motion, the solution of which leads to an eigenvalue problem.

In the absence of wind flow (i.e. zero wind speed) it has been shown by Lwambuka (1988) that the identification yields system parameter matrices $\underline{M}_s, \underline{D}_s, \underline{K}_s$ (natural model). Model parameters identified under the influence of wind (aerodynamic model) are found to differ considerably from those obtained in still air. The influence of wind (i.e. wind load parameters) can be extracted by use of eq. (4) as functions of wind speed.

3. SYSTEM PARAMETER IDENTIFICATION TECHNIQUE

3.1 Test Model

The identification of parameters is based on the measurement of acceleration response signals by use of accelerometers which are mounted on the test model at locations which correspond to the degrees of freedom. The test model selected for this purpose was a thin plate, elastically suspended to allow three degrees of freedom as shown in fig.(1). The model was selected to comply with the classical airfoil idealization (=thin plate) from which theoretical wind loads be derived using the methodology as described by Theodorsen (1935) and Lwambuka (1988).

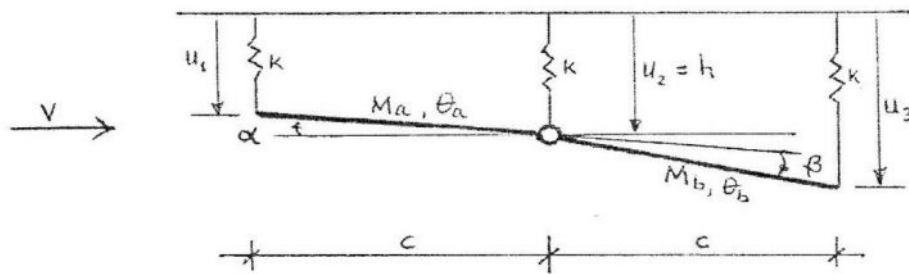


Fig.1: Elastically Restrained Flat Plate Model

With

- M_a, M_b = flat plate masses
- Θ_a, Θ_b = flat plate moment of inertia
- k = elastic stiffness
- c = reference geometrical length
- v = wind speed
- u_1, u_2, u_3 = vertical coordinates
- h, α, β = classical coordinates

The author adopted the vertical coordinate system which he found to be adequate for response measurements by use of accelerometers. In fig.2 is a plan view of the test model showing positioning of accelerometers, whereas the model suspension in wind tunnel is shown in fig. 3

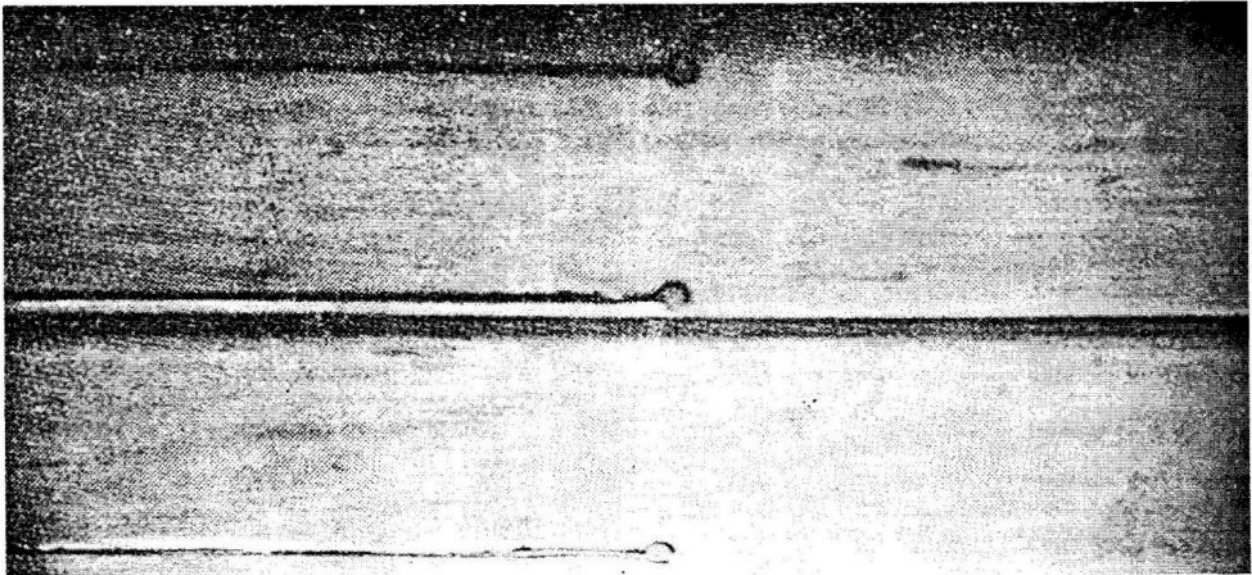


Fig.2: Test Model

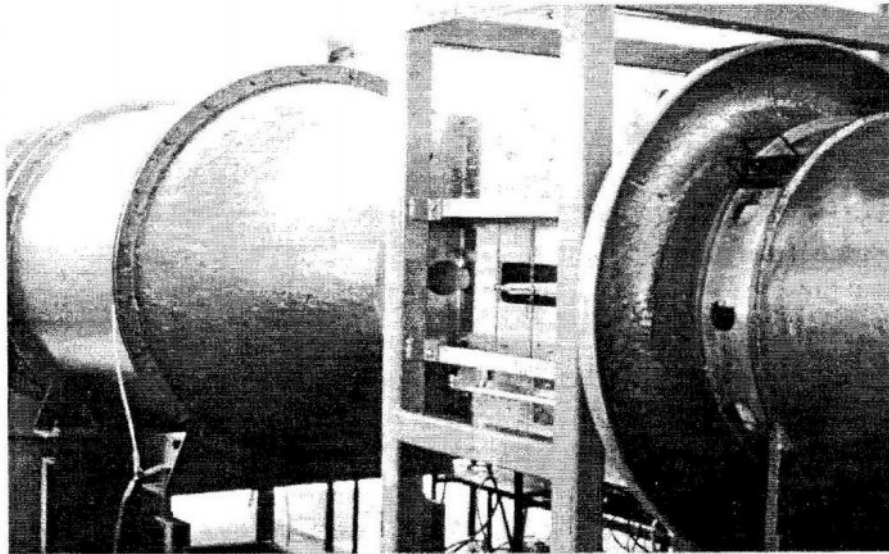


Fig.3: Model Suspended in Wind Tunnel

3.2 Response Data Processing

The accumulated response signals are first interpolated to form Lagrange's polynomial function of 7th order. In order to minimize the noise modes normally associated with the measurements, the polynomial function is integrated numerically. Henceforth, the terminology "integrated acceleration" is adopted. But since the application of eq.(3) requires also the knowledge of the velocity and displacement functions, two additional successive integrations are necessary. Therefore, after three numerical integration processes of the acceleration response, eq.(3) leads to eq.(5) which is known as "the identification equation":

$$\underline{M}_s \dot{\underline{U}}_e + \underline{D}_s \underline{U}_e + \underline{K}_s \bar{\underline{U}}_e = \underline{Q}, \quad e = 1, k \quad (5)$$

Where the response vectors are designated:

- $\dot{\underline{U}}$ = integrated acceleration
- \underline{U} = integrated velocity and
- $\bar{\underline{U}}$ = integrated displacement.

If for each measuring station on the test model, s response signals have been recorded, then the total number of identification equations k obtained and represented by eq.(5) will be

$$k = \frac{s}{m}, \quad (6)$$

Whereby m , the polynomial interpolation order, equals 7.

Eq.(5) as it stands is a product of three integration processes and therefore contains 3 unknown constants, i.e. the initial response values. Determination of the 3 integration constants, which represent the initial conditions, can be avoided by employing a differentiation concept, which is prescribed by Badenhausen (1985). The differentiation process reduces the number of identification equations by 2 to form eq.(7):

$$\underline{M}_s \dot{\underline{U}}_e + \underline{D}_s \underline{U}_e + \underline{K}_s \bar{\underline{U}}_e = \underline{Q}, \quad e = 1, p \quad (7)$$

with

$$p = k - 2$$

3.3 Response Data Quantity

In order to facilitate the datum process as prescribed above, the collection of a sufficient quantity of data constitutes the first objective of the test. The accuracy of identification depends on the degree of indeterminacy of eq.(7), which is given by the number of identification equations, p . One must therefore respond to the basic question: How many response signals will be required to produce a minimum number of p equations?

The quantity of data procured at each measuring station is given by

$$S = \frac{T_m}{\Delta t} \quad (8)$$

whereby

Δt = recording time interval (in seconds)

T_m = test duration (in seconds)

Experience gained through the investigations of Badenhausen (1985) and Lwambuka (1988), recommends that the rate of signal recording should exceed at least 4 times the highest natural frequency of the vibrating system. From the model specifications of Fig.(1), the mass and stiffness matrices can be derived to obtain the form:

$$M_s = \begin{bmatrix} \frac{M_a + \Theta_a}{4} + \frac{\Theta_a}{c^2} & \frac{M_a - \Theta_a}{4} - \frac{\Theta_a}{c^2} & 0 \\ \frac{M_a - \Theta_a}{4} - \frac{\Theta_a}{c^2} & \frac{1}{4} \left(M_a + M_b + \frac{1}{c^2(\Theta_a + \Theta_b)} \right) & \frac{M_b - \Theta_b}{4} - \frac{\Theta_b}{c^2} \\ 0 & \frac{M_b - \Theta_b}{4} - \frac{\Theta_b}{c^2} & \frac{M_b + \Theta_b}{4} + \frac{\Theta_b}{c^2} \end{bmatrix} \quad (9)$$

$$K_s = \begin{bmatrix} k & 0 & 0 \\ 0 & k & 0 \\ 0 & 0 & k \end{bmatrix} \quad (10)$$

On setting up the experiment the following data were established:

$$\begin{aligned} M_a = M_b &= 1.376 \cdot 10^{-4} [kNm s^{-2}] \\ c &= 0.093 [m] \\ \Theta_a = \Theta_b &= 1.570 \cdot 10^{-7} [kNm s^{-2}] \\ k &= 0.288 [kNm^{-1}] \end{aligned}$$

for which the vibration modes are characterized by the three natural frequencies:

$$f_1 = 7.53, f_2 = 11.57, f_3 = 14.48 [HZ] \quad (11)$$

with

$$f = \frac{\omega}{2\pi} \quad (12)$$

If η_f is defined to represent the ratio between the rate of recording, f_A , and the highest natural frequency of the system, f_3 , then the recommendations stated above implies that

$$\eta_f, \min = \frac{f_A}{f_3} = \frac{1}{m \cdot \Delta t \cdot f_3} \geq 4 \quad (13)$$

A recording time interval of say

$$\Delta t = 0.002 \text{ sec}$$

is arbitrarily selected. Hence with f_3 and $m = 7$ we obtain

$$\eta_f = 4.93.$$

Observing that the vibrating system of fig.1 has three recording stations as portrayed in fig.(2), Δt specifies a recording capacity requirement of $f_A = 500$ signals/sec on all the three channels simultaneously.

The duration of the test T_m can be obtained from recommendations on experiences set forth by Badenhausen (1985). In general, it should

exceed about 10 times that of the period of the lowest natural frequency. In our case, the duration of the test is therefore obtained from f_1 as $T_m = 1.328 \text{ sec}$.

For practical purposes, the author recommends that the actual test duration T should be at least double the analytical duration T_m :

$$T = 2T_m \quad (14)$$

The recommendation in eq.(14) allows for a free selection of the amplitude \ddot{U}_0 as reference for the analysis fig.4.

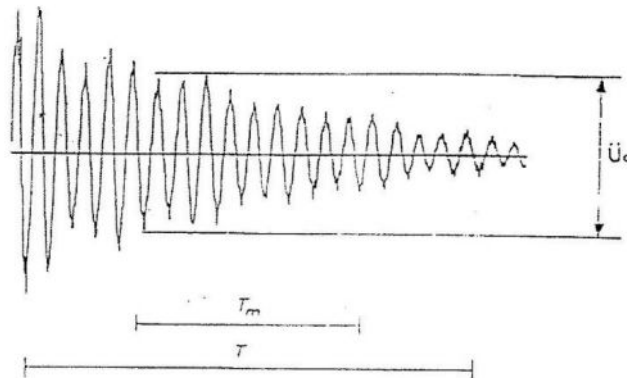


Fig.4: The desirable duration T_m and the actual duration T of the vibration test.

4. WIND LOAD PARAMETERS

After numerically processing the procured response signals to form eq.(7), the identification of system parameters \underline{M} , \underline{D} , \underline{K} follows directly by use of the time domain methodology as described by Badenhausen in 1985 and Lwambuka in 1988. With eq.(4), wind

load parameter matrices \underline{M}_w , \underline{D}_w , \underline{K}_w can be extracted and eq.(1) becomes definitive. For evaluation purposes, we seek a classical presentation of the wind load parameters by transforming eq.(1) into classical coordinates $\approx \underline{U}$. A transformation matrix is defined as follows:

$$\underline{\mathbf{T}} = \begin{matrix} & u_1 & u_2 & u_3 \\ \mathbf{h} & \begin{bmatrix} 0 & 1 & 0 \\ -\frac{1}{c} & \frac{1}{c} & 0 \\ \frac{1}{c} & -\frac{2}{c} & \frac{1}{c} \end{bmatrix} \\ \mathbf{\beta} & \end{matrix} \quad (15)$$

so that

$$\begin{aligned} \underline{\mathbf{M}} &= \underline{\mathbf{T}}^{-T} \underline{\mathbf{M}} \underline{\mathbf{T}}^{-1} \\ \underline{\mathbf{D}} &= \underline{\mathbf{T}}^{-T} \underline{\mathbf{D}} \underline{\mathbf{T}}^{-1} \\ \underline{\mathbf{K}} &= \underline{\mathbf{T}}^{-T} \underline{\mathbf{K}} \underline{\mathbf{T}}^{-1} \end{aligned} \quad (16)$$

$$\underline{\mathbf{U}} \approx \underline{\mathbf{T}} \underline{\mathbf{U}} \quad (17)$$

Introducing an arbitrary, dimensional factor matrix, F_v of the form

$$F_v = \begin{bmatrix} Lpv^2c & 0 & 0 \\ 0 & Lpv^2c^2 & 0 \\ 0 & 0 & Lpv^2c^2 \end{bmatrix} \quad (18)$$

Eq.(1) can be re-written in dimensionless wind load matrices $\underline{\mathbf{M}}_w^*, \underline{\mathbf{D}}_w^*, \underline{\mathbf{K}}_w^*$ as well as dimensionless

response vectors $\underline{\mathbf{U}}_w^*, \underline{\mathbf{U}}_s^*, \underline{\mathbf{U}}^*$ given by eq.(19) below

$$\underline{\mathbf{M}}_s^* \underline{\mathbf{U}}_s^* + \underline{\mathbf{D}}_s^* \underline{\mathbf{U}}_s^* + \underline{\mathbf{K}}_s^* \underline{\mathbf{U}}_s^* = \underline{\mathbf{F}}_v \left[\underline{\mathbf{M}}_w^* \underline{\mathbf{U}}_w^* + \underline{\mathbf{D}}_w^* \underline{\mathbf{U}}_w^* + \underline{\mathbf{K}}_w^* \underline{\mathbf{U}}_w^* \right] \quad (19)$$

The dimensionless response vectors of eq.(19) assume the form:

$$\underline{\mathbf{U}}_s^* = \begin{bmatrix} \ddot{\cdot} \\ \frac{c\dot{h}}{v^2} \\ \frac{c^2\ddot{a}}{v^2} \\ \frac{c^2\ddot{\beta}}{v^2} \end{bmatrix} \quad \underline{\mathbf{U}}_w^* = \begin{bmatrix} \dot{h} \\ \frac{c\dot{a}}{v} \\ \frac{c\dot{\beta}}{v} \end{bmatrix} \quad \underline{\mathbf{U}}^* = \begin{bmatrix} \frac{h}{c} \\ \alpha \\ \beta \end{bmatrix} \quad (20)$$

whereas the dimensionless wind load parameters are presented as follows:

$$\underline{M}^* \approx \begin{bmatrix} 1 & 0 & 0 \\ 0 & 1 & 0 \\ 0 & 0 & 1 \end{bmatrix} \begin{bmatrix} \approx^* & \approx & \approx \\ M_{w11}^* & M_{w12}^* & M_{w13}^* \\ \approx & \approx & \approx \\ M_{w21}^* & M_{w22}^* & M_{w23}^* \\ \approx & \approx & \approx \\ M_{w31}^* & M_{w32}^* & M_{w33}^* \end{bmatrix} \quad (21)$$

$$\underline{D}^* \approx \begin{bmatrix} \omega^* & 0 & 0 \\ 0 & \omega^* & 0 \\ 0 & 0 & \omega^* \end{bmatrix} \begin{bmatrix} \approx^* & \approx & \approx \\ D_{w11}^* & D_{w12}^* & D_{w13}^* \\ \approx & \approx & \approx \\ D_{w21}^* & D_{w22}^* & D_{w23}^* \\ \approx & \approx & \approx \\ D_{w31}^* & D_{w32}^* & D_{w33}^* \end{bmatrix} \quad (22)$$

$$\underline{K}^* \approx \begin{bmatrix} \omega^* & 0 & 0 \\ 0 & \omega^* & 0 \\ 0 & 0 & \omega^* \end{bmatrix} \begin{bmatrix} \approx^* & \approx & \approx \\ K_{w11}^* & K_{w12}^* & K_{w13}^* \\ \approx & \approx & \approx \\ K_{w21}^* & K_{w22}^* & K_{w23}^* \\ \approx & \approx & \approx \\ K_{w31}^* & K_{w32}^* & K_{w33}^* \end{bmatrix} \quad (23)$$

The matrix coefficients in Equations (21), (22) and (23) contain a total number of 27 elements. These are presented in this paper in Figures 5, 6 and 7 as real functions of the reduced frequency.

$$\omega^* = \frac{\omega c}{v} \quad (24)$$

Where

- ω = frequency of the vibrating system
- c = reference geometrical length
- v = wind speed

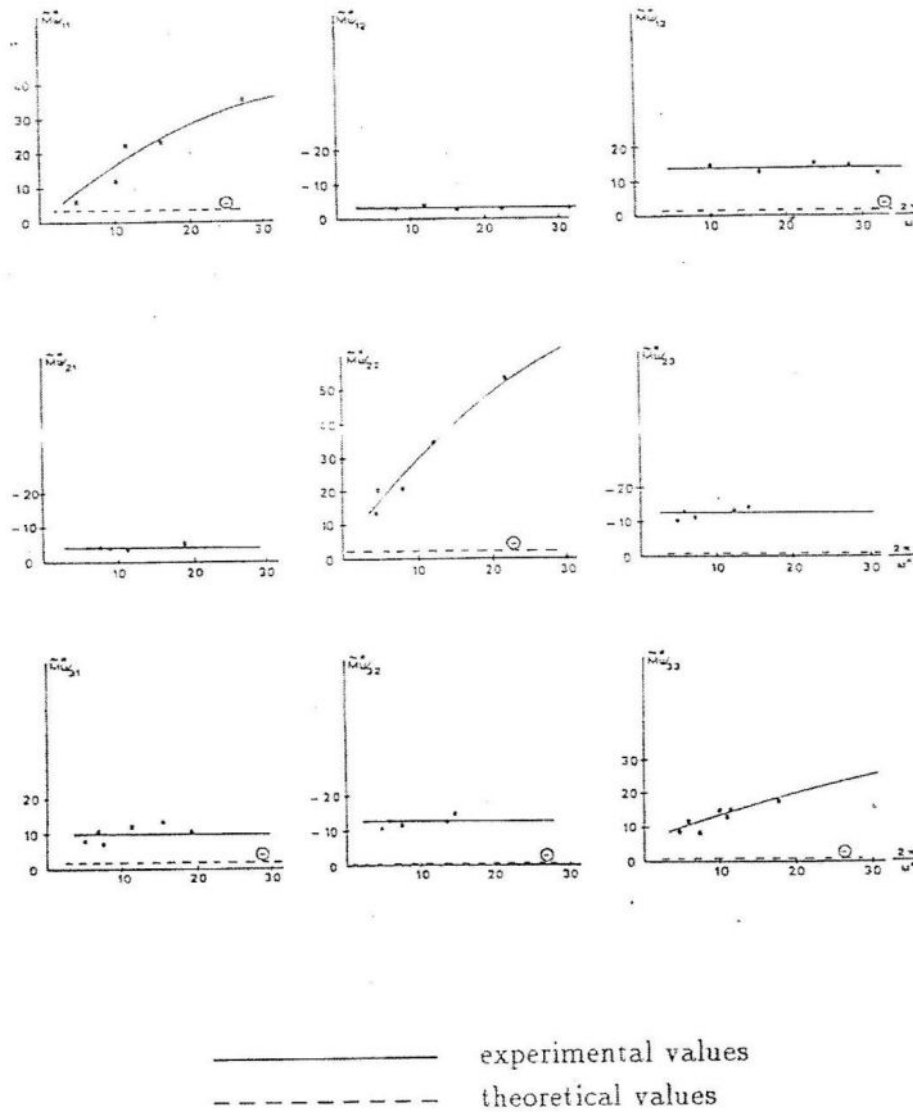


Fig.5: The Wind "Mass" Coefficients, M^*_{wij}

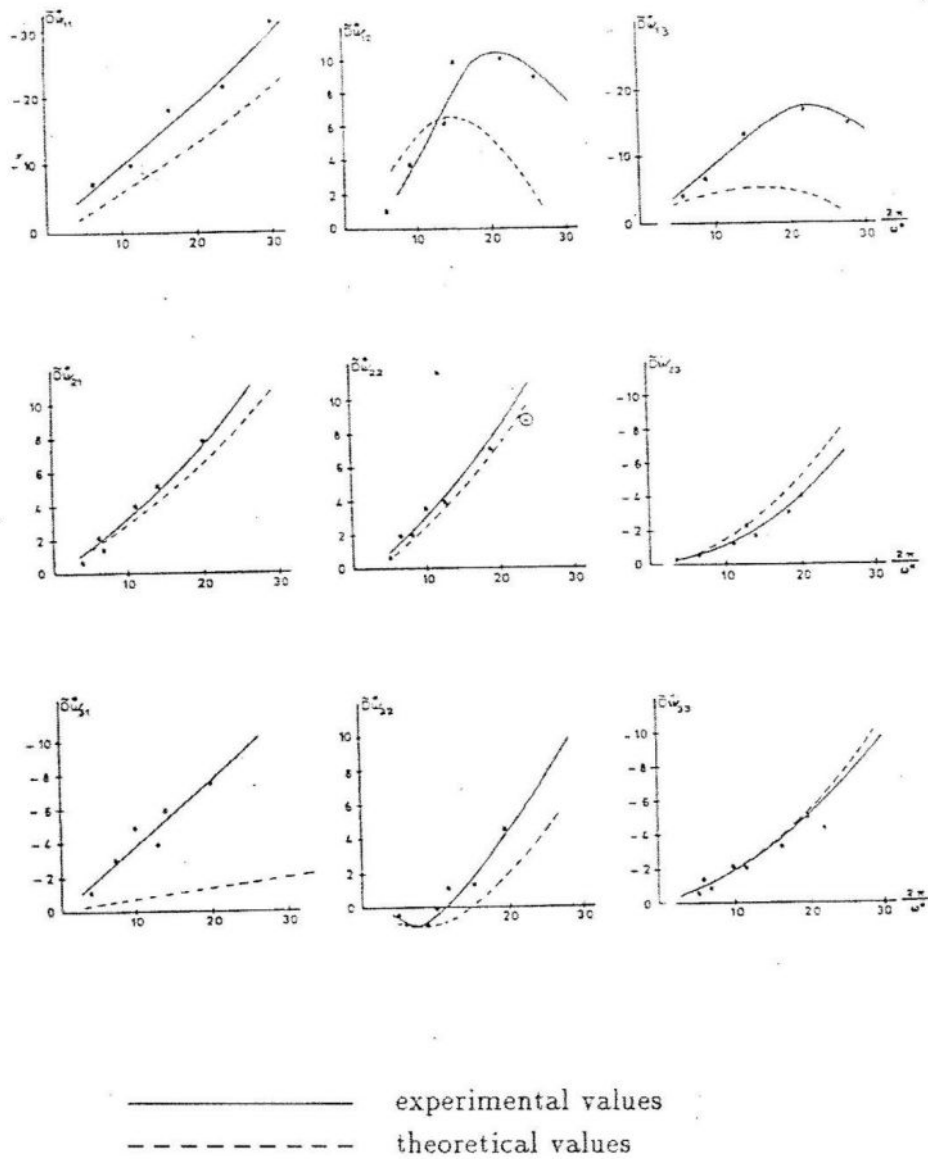
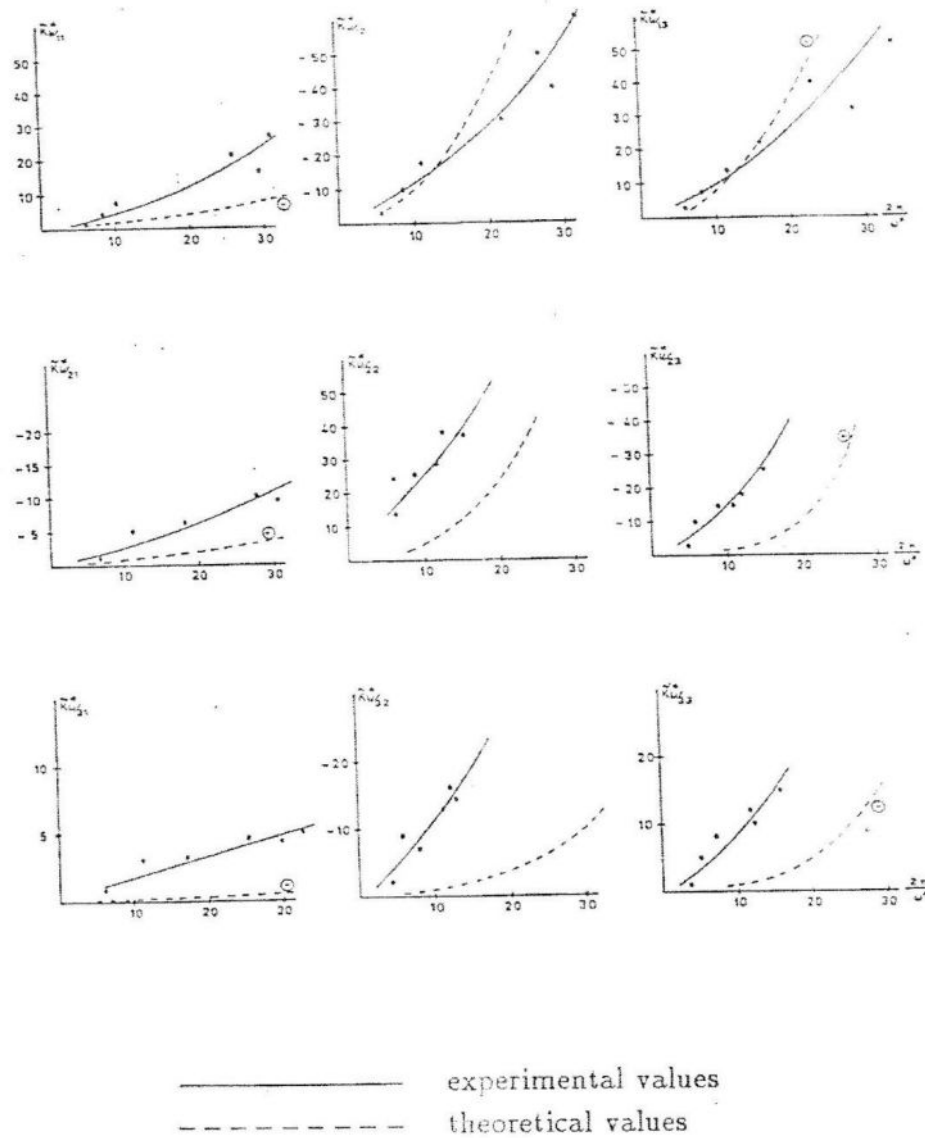


Fig.6: The wind "damping" coefficients, D^*_{wij}



≈
Fig.7: The wind "stiffness" Coefficients, K^*_{wij}

In Figures 5, 6 and 7, experimentally obtained functions of wind load coefficients under this method are being compared with real theoretical values, given in APPENDIX I, which are derived from the Theodorsen's complex functions.

5. RESULTS

Good agreement between experimental and theoretical results can be observed in Figs. 5, 6

and 7 for most of the coefficients. The deviations stem from the discrepancy of the test model from an ideal flat plate as well as the approximated overlapping of elastic supports and vertical coordinates (Figs. 1 and 2).

The accuracy of the method can further be verified by treating the model suspension as a real structure and solving the eigenvalue problem using experimentally obtained wind

load parameters. The solution presented in fig.8 provides the critical wind speed of

$$V_f = 9.8 \text{ m/s},$$

which defines the onset of flutter instability.

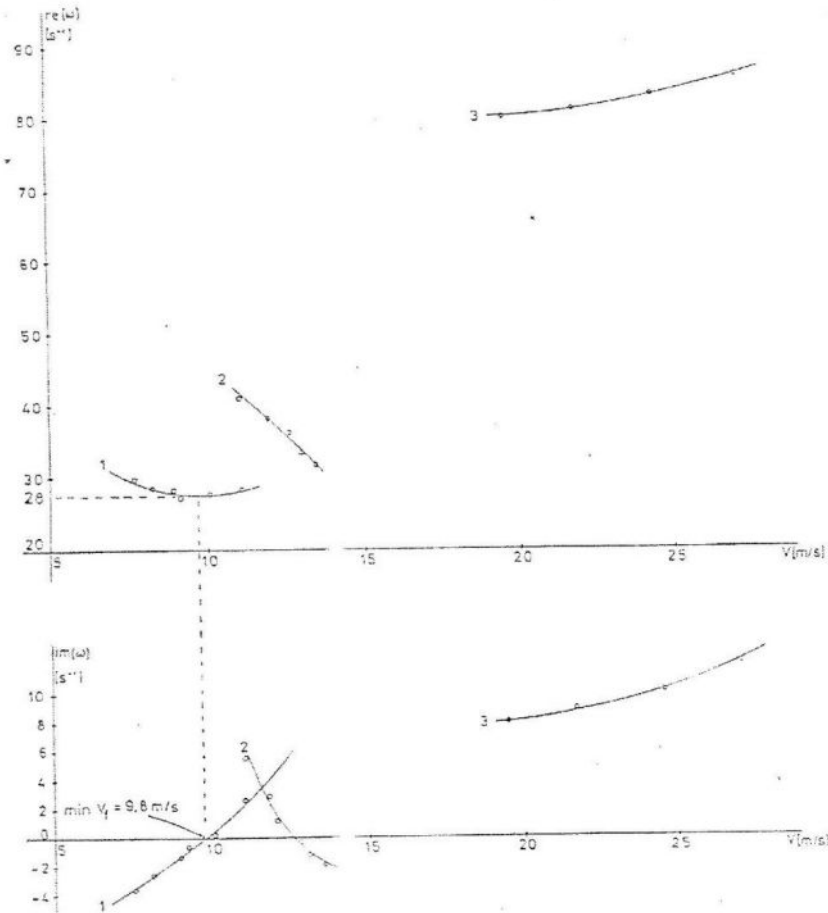


Fig.8: Determination of critical wind speed using experimentally obtained wind load parameters.

Repeating the analysis with theoretical wind load parameters leads to solutions presented in Fig. (9) with a critical wind speed of $V_f = 11.7 \text{ m/s}$,

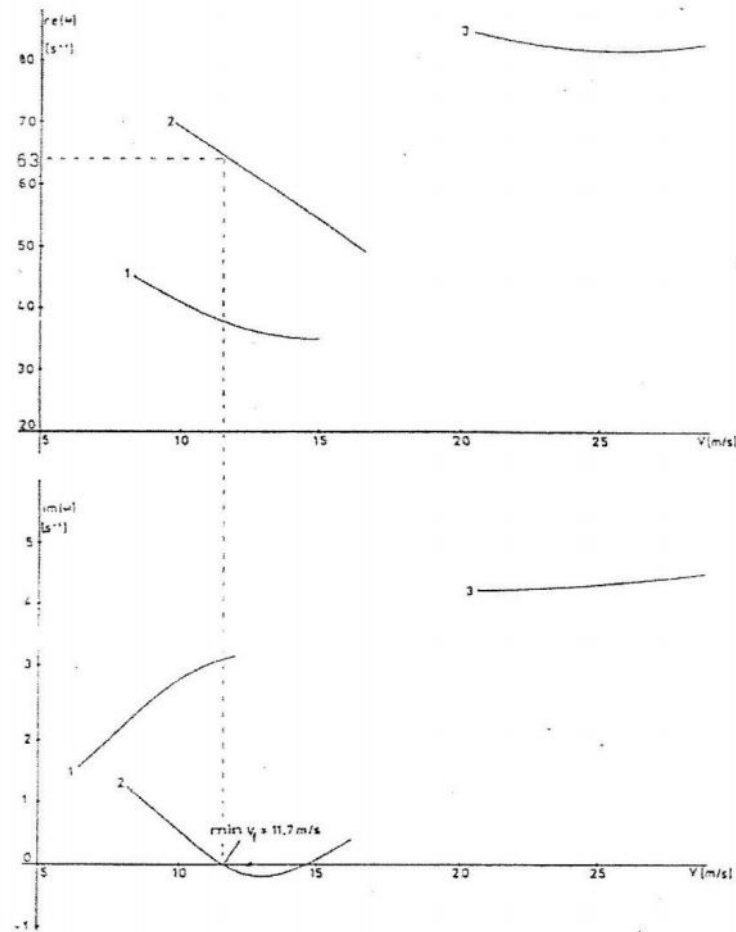


Fig.9: Determination of critical wind speed using theoretical wind load parameters (Appendix I)

The actual wind speed observed in the wind tunnel at which the model structure began to flutter was

$$V_f = 10.3 \text{ m/s},$$

Since the critical wind speed obtained by use of experimentally obtained wind loads is fairly close to reality, the accuracy of the new method would appear to be well justified.

6. CONCLUSIONS

On the basis of experimental results presented in this paper the following conclusions can be drawn.

1) The time domain identification technique provides an advanced approach for

experimental determination of wind load parameters.

2) In comparison with the conventional method, the new method not only reduces the technical requirement and experimental work on wind tunnel tests, but also increases the accuracy of results.

3) Although the method of approach presented in this paper bears the advantages over the conventional one, as pointed out under item 2 above, the data processing effort is extremely high. It requires the use of a high speed digital computer and a set of special software for data processing.

7. REFERENCES

Badenhausen, K., (1985). Identification der Modellparameter Elastomechanischer System aus Schwingungsversuchen. Dissertation, University of Kassel.

Ibrahim, S. R., (1973). A time Domain Model Model Test Technique Shock and Vibration Bulletin 43, part 4

Ibrahim, S. R., (1985). Advances in Time Domain Identification and Modeling of Structures Second International Symposium on Aeroelasticity and Structural Dynamics Technical University Aachen.

Ibrahim, S. R; and Mikulcik, E.C., (1976) The Experimental Determination of Vibration Parameters from Time Response Shock and Vibration Bulletin 46, P. 187 – 196.

Lwambuka, L., (1988). Berechnung Winderregter Schwingungen auf der Grundlage Experimenteller Parametridentifikation, Dissertation, University of Kassel.

Scanlan, R.H.; and Tomko, J.J., (1971). Airfoil and Bridge Deck Flutter Derivatives Proc. of the American Society of Civil Engineers, Journal of the Engineering Mechanics Division.

Scanlan, R. H., (1975). Theory of the Wind Analysis of Long-Span Bridges Based on Data obtained from Section Model Tests Proc. 4th Intern. Conf. on Wind Effects on Buildings and Structures.

Theodorsen, T., (1935). General Theory of Aerodynamic Instability and the Mechanism of Flutter National Advisory Committee of Aeronautics Report No. 496 (Original).

Appendix I: Theodorsen's Real Functions of Wind Load Parameters

The wind "mass" coefficients turn out to constant values of the form:

$$M_{w11}^* = -\pi$$

$$M_{w12}^* = 0$$

$$M_{w13}^* = -\frac{2}{3}$$

$$M_{w21}^* = 0$$

$$M_{w22}^* = -\frac{\pi}{8}$$

$$M_{w23}^* = -\frac{\pi}{16}$$

$$M_{w31}^* = -\frac{2}{3}$$

$$M_{w32}^* = -\frac{\pi}{16}$$

$$M_{w33}^* = -\pi\left(\frac{1}{32} + \frac{1}{2\pi^2}\right)$$

The wind "damping" coefficients will read

$$D_{w11}^* = -\frac{2\pi F}{\omega^*}$$

$$D_{w12}^* = -\pi\left\{\frac{1}{w^*} + \frac{F}{w^*} + \frac{2G}{w^{*2}}\right\}$$

$$D_{w13}^* = -\pi\left\{\frac{1}{2w^*} + \frac{F}{2w^*} + \frac{2F}{w^*\pi} + \frac{2G}{w^{*2}\pi} + \frac{G}{w^{*2}}\right\}$$

$$D_{21}^* = -\frac{\pi F}{w^*}$$

$$D_{w22}^* = -\pi\left\{\frac{1}{2w^*} - \frac{F}{2w^*} - \frac{G}{w^{*2}}\right\}$$

$$D_{w23}^* = -\pi\left\{\frac{2}{3\pi w^*} + \frac{1}{4w^*} - \frac{F}{\pi w^*} - \frac{F}{4w^*} - \frac{G}{\pi w^{*2}} - \frac{G}{w^{*2}}\right\}$$

$$D_{w31}^* = \pi\left\{\frac{F}{2w^*} - \frac{2F}{\pi w^*}\right\}$$

$$D_{w32}^* = -\pi\left\{\frac{2}{3\pi w^*} - \frac{1}{4w^*} - \frac{F}{\pi w^*} + \frac{F}{4w^*} - \frac{2G}{\pi w^{*2}} + \frac{G}{2w^{*2}}\right\}$$

$$D_{w33}^* = -\pi\left\{\frac{1}{8w^*} - \frac{1}{2\pi w^*} - \frac{\left(2 - \frac{\pi}{2}F\right)}{4\pi w^*} - \frac{\left(2 - \frac{\pi}{2}\right)}{\pi^2 w^*} - \frac{\left(2 - \frac{\pi}{2}\right)G}{\pi^2 w^{*2}} - \frac{\left(2 - \frac{\pi}{2}\right)G}{2\pi w^{*2}}\right\}$$

Whereas the wind "stiffness" coefficients take the form:

$$K_{w11}^* = \frac{2\pi G}{w^*}$$

$$K_{w12}^* = -\pi \left\{ \frac{2F}{w^{*2}} - \frac{G}{w^*} \right\}$$

$$K_{w13}^* = -\pi \left\{ \frac{2F}{\pi w^{*2}} + \frac{F}{w^{*2}} - \frac{G}{2w^*} - \frac{2G}{\pi w^*} \right\}$$

$$K_{w21}^* = -\frac{\pi G}{w^*}$$

$$K_{w22}^* = \pi \left\{ \frac{F}{w^{*2}} - \frac{G}{2w^*} \right\}$$

$$K_{w23}^* = -\pi \left\{ \frac{1}{\pi w^{*2}} - \frac{F}{\pi w^{*2}} - \frac{F}{2w^{*2}} + \frac{G}{4w^*} + \frac{G}{\pi w^*} \right\}$$

$$K_{31}^* = \pi \left\{ \frac{2G}{\pi w^*} - \frac{G}{2w^*} \right\}$$

$$K_{w32}^* = \pi \left\{ \frac{G}{\pi w^*} - \frac{G}{4w^*} - \frac{2F}{\pi w^{*2}} + \frac{F}{2w^{*2}} \right\}$$

$$K_{33}^* = \pi \left\{ \frac{1}{\pi^2 w^{*2}} - \frac{1}{2\pi w^{*2}} - \frac{\left(2 - \frac{\pi}{2}\right)F}{\pi^2 w^{*2}} - \frac{\left(2 - \frac{\pi}{2}\right)F}{2\pi w^{*2}} + \frac{\left(2 - \frac{\pi}{2}\right)G}{4\pi w^*} + \frac{\left(2 - \frac{\pi}{2}\right)G}{\pi^2 w} \right\}$$

with

F = The real part of Theodorsen – Function
 G = The imaginary part of Theodorsen – Function

Appendix II: List of Symbols

- * Notation for dimensionless parameter
- c Reference geometrical length
- k Spring constant
- L Profile length
- ω Vibration frequency
- F Real part of Theodorsen – Function
- G Imaginary part of Theodorsen – Function

$M_{w_{ij}}^*, D_{w_{ij}}^*, K_{w_{ij}}^*$ Wind Load Coefficients

\approx

\underline{U} Displacement vector in classical coordinates h, α, β

\underline{U} Displacement vector in vertical coordinates u_1, u_2, u_3

\underline{T} Transformation matrix

$\underline{\tilde{M}}_s, \underline{\tilde{D}}_s, \underline{\tilde{K}}_s$	System matrices based on $\underline{\tilde{U}}$
$\underline{M}_s, \underline{D}_s, \underline{K}_s$	System matrices based on \underline{U}
\underline{F}_v	Dimensional factor matrix
$\underline{\tilde{M}}_w, \underline{\tilde{D}}_w, \underline{\tilde{K}}_w$	Wind load matrices based on $\underline{\tilde{U}}$
$\underline{M}_w, \underline{D}_w, \underline{K}_w$	Wind load matrices based on \underline{U}